about one-tenth as much as was detected 3 days after cointroduction with HMG-1. When the DNA was cointroduced with BSA, it was not detectable by Southern hybridization after 12 days.
16. To standardize the amount of poly(A)$^+$ RNA in each sample, the filter was hybridized with ^{32}P-labeled rat albumin cDNA probe. The density ratio of SV40 large T antigen poly(A)$^+$ RNA to rat albumin poly(A)$^+$ RNA was compared.
17. F. Szoka and D. Papahadjopoulos, *Proc. Natl. Acad. Sci. U.S.A.* **75**, 145 (1978).
18. J. Bentley-Lawrence *et al.*, *Cell* **52**, 51 (1988).
19. N. Fregien and N. Davidson, *Gene* **48**, 1 (1986).
20. C. M. Gorman, L. F. Moffat, B. H. Howard, *Mol. Cell. Biol.* **2**, 1044 (1982).
21. E. M. Southern, *J. Mol. Biol.* **98**, 503 (1975).
22. T. Maniatis, E. F. Fritsch, J. Sambrook, *Molecular Cloning: A Laboratory Manual* (Cold Spring Harbor Laboratory, Cold Spring Harbor, NY, 1982).
23. M. Yamaizumi, T. Uchida, Y. Okada, M. Furusawa, H. Mitsui, *Nature* **273**, 782 (1978).
24. J. M. Chirgwin, R. J. Pryzybyla, R. J. MacDonald, W. J. Rutter, *Biochemistry* **18**, 5294 (1979).
25. H. Aviv and P. Leder, *Proc. Natl. Acad. Sci. U.S.A.* **69**, 1408 (1972).
26. We thank Y. Okada, Institute for Molecular and Cellular Biology, for his advice and encouragement and P. Berg for the gift of pBR-SV40. Supported by grants from the Ministry of Education, Science and Culture of Japan, and the Foundation for Promotion of Cancer Research backed by Japan Shipbuilding Industry Foundation.

16 August 1988; accepted 20 October 1988

Isolation and Expression of Functional High-Affinity Fc Receptor Complementary DNAs

JANET M. ALLEN AND BRIAN SEED

Human and murine mononuclear phagocytes express a high-affinity receptor for immunoglobulin G that plays a central role in macrophage antibody-dependent cellular cytotoxicity and clearance of immune complexes. The receptor (FcRI) may also be involved in CD4-independent infection of human macrophages by human immunodeficiency virus. This report describes the isolation of cDNA clones encoding the human FcRI by a ligand-mediated selection technique. Expression of the cDNAs in COS cells gave rise to immunoglobulin G binding of the expected affinity and subtype specificity. RNA blot analysis revealed expression of a 1.7-kilobase transcript in macrophages and in cells of the promonocytic cell line U937 induced with interferon-γ. The extracellular region of FcRI consists of three immunoglobulin-like domains, two of which share homology with low-affinity receptor domains.

THE MACROPHAGE-SPECIFIC RECEPTOR (FcRI) for the constant region (Fc) of immunoglobulin G (IgG) plays a central role in antibody-dependent cellular cytotoxicity and clearance of immune complexes (*1*). FcRI has been hypothesized to participate in antibody dependent infection of macrophages by dengue virus and human immunodeficiency virus (HIV) (*2*). Considerable recent success has attended the identification of cDNAs that encode low-affinity Fc receptors (*3, 4*). However, the cDNAs encoding the high-affinity receptor for IgG_1 have eluded detection. In this report, three independent cDNAs for FcRI were isolated by transient COS cell expression and affinity selection (*4, 5*). DNA sequence analysis revealed that the extracellular region comprised three immunoglobulin domains. The first two bear homology with the low-affinity Fc receptors, whereas the third domain is unique and may be responsible for the higher affinity of the receptor.

A cDNA library was constructed from polyadenylated [poly(A)$^+$] RNA obtained from cells of a single patient undergoing extracorporeal interleukin-2 induction therapy. The library was introduced into COS cells by DEAE dextran transfection. Cells expressing Fc receptors were recovered 48 hours later by incubating them with mouse Ig and panning on dishes coated with affinity-purified goat antibody to mouse Ig (Cappel). Episomal DNA was recovered from adherent cells by the Hirt procedure (*6*), amplified in *Escherichia coli*, and reintroduced into COS cells by spheroplast fusion. After four rounds, DNA was prepared from individual colonies and transfected into COS cells. Expression of Fc receptors was determined by indirect immunofluorescence after 48 hours. Three clones, p135, p90, and p98/X2 were selected for further study.

Indirect immunofluorescence showed that COS cells transfected separately with the three clones bound human IgG, human IgG Fc fragments, murine IgG2a, and the FcRI-specific monoclonal antibodies (MAb), 32.2 (*7*) and 22.2 (*8*). Fluorescein-conjugated goat antibodies, human IgA, IgM, IgD, and $F(ab')_2$ fragments, as well as murine IgG_1, IgG_{2b}, IgM, and the FcRII-specific MAb, IV.3 (*9*) did not react. COS cells expressing one of the cDNA clones formed rosettes with bovine erythrocytes coated with rabbit IgG, but not with IgM (*10*).

IgG-agarose adsorption (*4*) of surface-labeled COS cells transfected with p135 and p90 showed a single species of relative molecular size 70 kD, whereas similar treatment of cells transfected with p98/X2 gave a band of 67 kD (Fig. 1). A slightly larger protein of 75 kD was adsorbed from untreated and interferon-γ (IFN-γ)–treated U937 cells. The smaller mass observed in COS cells is consistent with the reduced masses observed for other surface antigens expressed in COS cells (*5*).

Scatchard analysis (*11*) of the binding of radiolabeled IgG_1 to COS cells transfected with each of the three clones revealed 5×10^5 to 10×10^5 binding sites with similar association constants of $\approx 5 \times 10^7 M^{-1}$ (Fig. 2A). The specificity of the three clones, measured by displacement titrations of labeled IgG_1, showed the same rank order for human and murine subtypes in all three clones. In agreement with in vivo data (*1*), human IgG_1 and IgG_3 showed equipotent displacement of radiolabeled IgG_1, whereas human IgG_2 and IgG_4 were less effective (Fig. 2B). Among the murine IgG subtypes, the highest affinity was displayed by IgG_{2a} (Fig. 2C), consistent with previous studies. Murine IgG_3 also displaced binding of radiolabeled human IgG_1 to a lesser extent, whereas murine IgG_{2b} and IgG_1 were ineffectual (Fig. 2C).

RNA blot analysis (Fig. 3) with the p135 probe showed a single 1.7-kb transcript in RNA prepared from monocytes, placenta [a rich source of macrophage transcripts (*4*)], and the cells from which the library was generated. No transcripts were observed from RNA derived from similar cell preparations from two other patients. In the

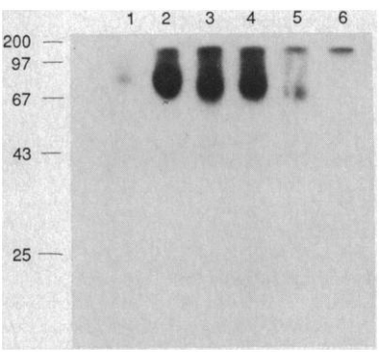

Fig. 1. IgG-agarose adsorption of surface ^{125}I-labeled cells. (Lane 1) U937 cells; (lane 2) U937 cells stimulated for 48 hours with recombinant IFN-γ (10 ng/ml) (Hoechst); (lanes 3 to 6) COS cells transfected with: p135 (lane 3), p90 (lane 4), p98/X2 (lane 5), and vector (lane 6). Cells were labeled by the lactoperoxidase method, lysed, and adsorbed to human IgG-agarose (Sigma) as described elsewhere (*4*). Markers in kilodaltons.

J. M. Allen, Department of Molecular Biology and Department of Neurology, Massachusetts General Hospital, Boston, MA 02114.
B. Seed, Department of Molecular Biology, Massachusetts General Hospital, Boston, MA 02114.

promonocytic cell line U937, two transcripts of 1.7 and 1.6 kb were seen. The abundance of both transcripts increased upon culture of the cells in the presence of IFN-γ, which has previously been reported to induce FcRI surface expression (*12*). The increase was apparent in the first hour and reached a peak between 6 and 12 hours. In contrast, the increase in surface expression of the receptor was measurable only 12 hours after IFN-γ treatment and was highest at 24 hours (*10*). The lag between induction of the mRNA and expression of the protein suggests the involvement of posttranslational processes, possibly including compartmentalization.

Blot hybridization of genomic DNA cleaved with restriction enzymes recognizing a single site in the cDNA revealed a pattern consistent with at most two genes, closely linked (*10*).

The p135 and p90 cDNA inserts consist of 1322 and 1295 nucleotides, respectively. Both inserts terminate in poly(A) residues, which are preceded by a typical AATAAA polyadenylation motif. The two clones are almost identical, differing only in the length of the 5′ untranslated region and the number of residues between the polyadenylation motif and the poly(A) tract. Two polymorphisms were found within the open reading frame that resulted in conservative amino acid substitutions at positions 25 (p135, Ser; p90, Thr) and 58 (p135, Leu; p90, Val). The substitutions had no effect on

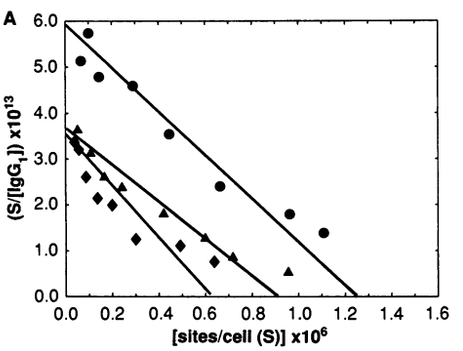

Fig. 2. Ligand-binding analysis of transfected COS cells. (**A**) Scatchard analysis of the binding of ^{125}I-labeled human IgG_1 to transfected COS cells (*11*) Results are typical of two to four replications. Data obtained with p135-transfected COS cells (●), p90-transfected cells (▲), and p98/X2-transfected cells (♦). (**B** and **C**) IgG subtype displacement analysis. The fraction of ^{125}I-labeled IgG_1 tracer bound is plotted as a function of the indicated concentrations of nonradioactive IgGs. (B) Displacement by human IgG subtypes 1, 2, 3, and 4. (C) Displacement by murine IgG subtypes 1, 2a, 2b, and 3. Binding of ligand and separation of bound and free fractions was carried out as in (A).

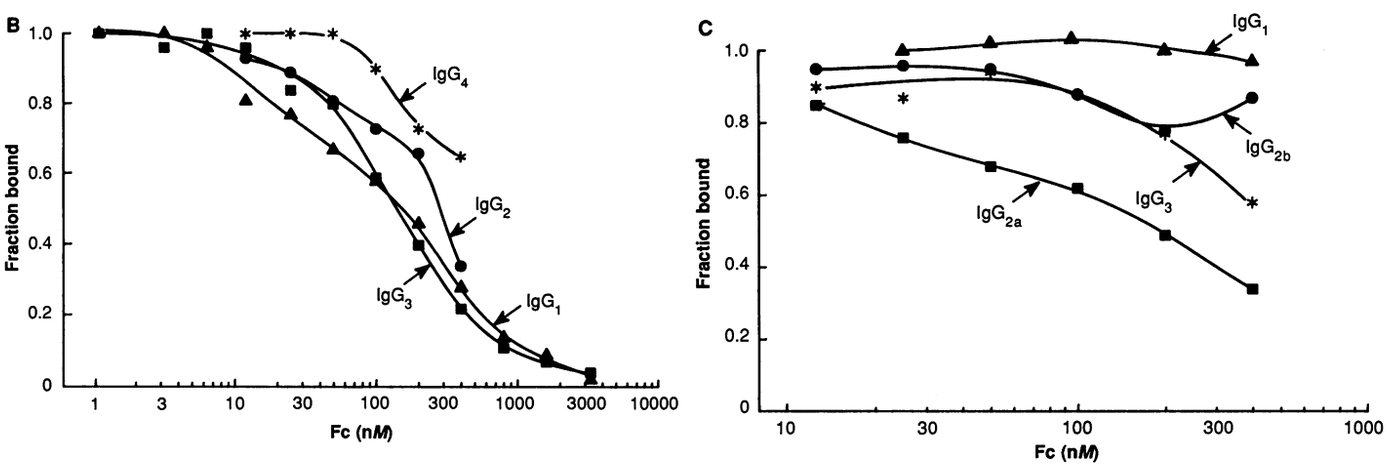

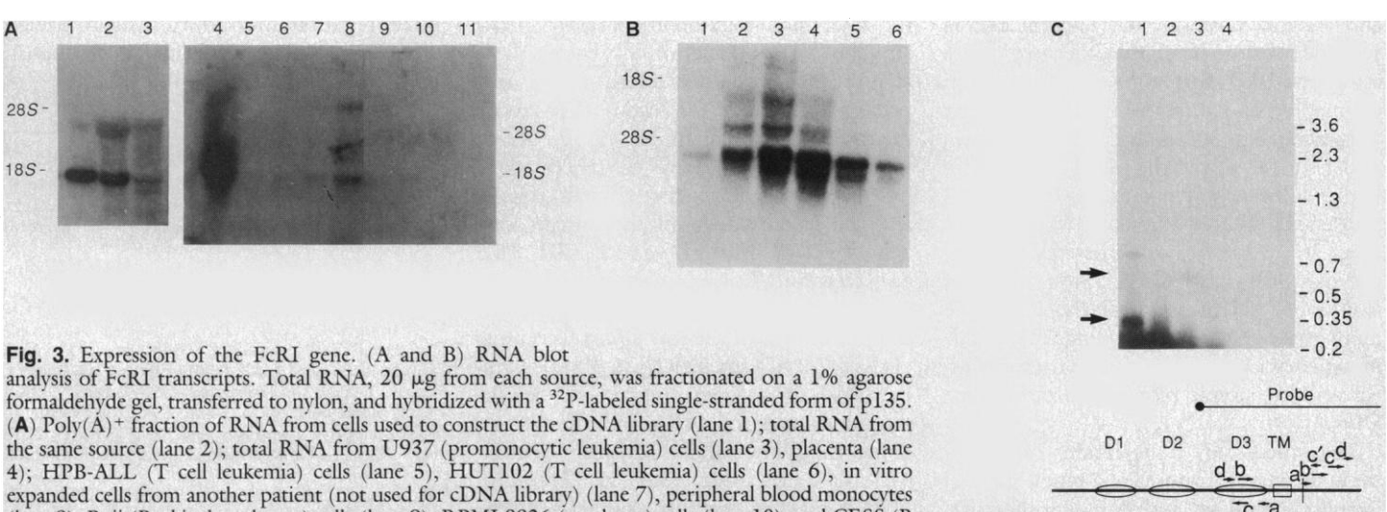

Fig. 3. Expression of the FcRI gene. (A and B) RNA blot analysis of FcRI transcripts. Total RNA, 20 μg from each source, was fractionated on a 1% agarose formaldehyde gel, transferred to nylon, and hybridized with a ^{32}P-labeled single-stranded form of p135. (**A**) Poly(A)$^+$ fraction of RNA from cells used to construct the cDNA library (lane 1); total RNA from the same source (lane 2); total RNA from U937 (promonocytic leukemia) cells (lane 3), placenta (lane 4); HPB-ALL (T cell leukemia) cells (lane 5), HUT102 (T cell leukemia) cells (lane 6), in vitro expanded cells from another patient (not used for cDNA library) (lane 7), peripheral blood monocytes (lane 8), Raji (Burkitt lymphoma) cells (lane 9), RPMI 8826 (myeloma) cells (lane 10), and CESS (B lymphoblastoid) cells (lane 11). Positions of the 18*S* and 28*S* rRNA are indicated. (**B**) IFN-γ stimulation of FcRI transcripts in U937 cells. Cells were either unstimulated (lane 1), or treated with recombinant IFN-γ (10 ng/ml) (Hoechst) for 1 hour (lane 2), 3 hours (lane 3), 6 hours (lane 4), 12 hours (lane 5), or 24 hours (lane 6). (**C**) S1 nuclease protection assay. Radiolabeled Bst EII–Bam HI fragment from p98/X2 was hybridized with RNA from IFN-γ–stimulated U937 cells (FcRI$^+$) (lane 1) and HUT-102 cells (FcRI$^-$) (lane 2). A similar fragment from p90 was hybridized with RNA from IFN-γ–stimulated U937 cells (lane 3) and HUT-102 (lane 4). Markers in kilobases. The three extracellular Ig-like domains are labeled D1, D2, and D3, and the transmembrane domain is marked TM. The point of divergence between the p98/X2 cDNA and p90 is marked by a vertical line. The repeated motifs that comprise the 3′ end of p98/X2 are indicated by arrows.

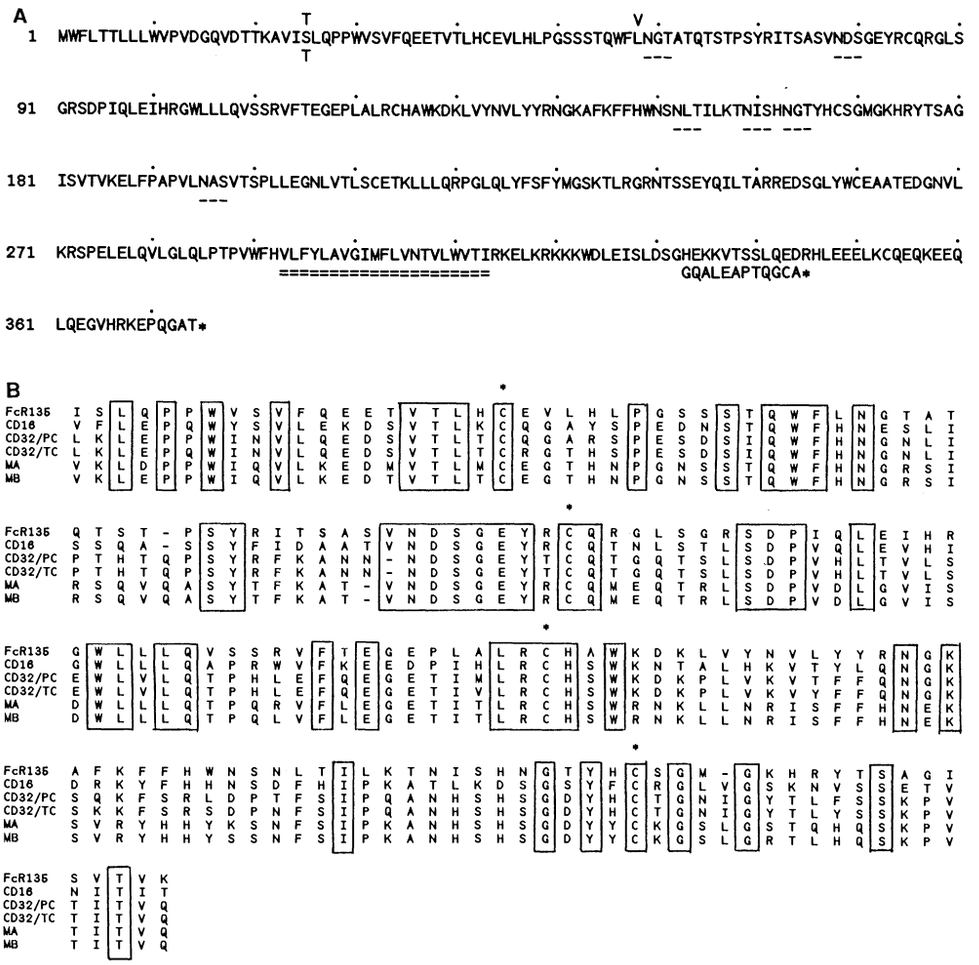

Fig. 4. Amino acid sequence and homology with low-affinity receptors. (**A**) Translated amino acid sequence (*16*) of the FcRI sequence. The sequence of the coding region of p135 is shown, and the two amino acid differences predicted for the p90 clone are shown above the sequence. The amino acids that differ in the p98/X2 clone are shown below the sequence. Sites of potential N-linked glycosylation are underlined and the hydrophobic membrane–spanning domain is double-underlined. The nucleotide sequences were obtained by dideoxy-chain termination (*17*) by the use of specific oligonucleotide primers and have been deposited in GenBank (accession numbers M21090 and M21091 for p135 and p98, respectively). (**B**) Alignment of the first two immunoglobulin domains of FcRI with those of the low-affinity receptors (*3, 4*): FcRIII (CD16), two forms of FcRII (CD32/PC, PC23; and CD32/TC, TC9), the α form of the murine Fcγ2b/1 receptor (MA) and the β form of the murine Fcγ2b/1 receptor (MB), produced by the ALIGN program. Conserved amino acids are boxed, and conserved cysteine residues are marked with an asterisk.

affinity or subtype specificity. The threonine polymorphism is associated with a Bcl I restriction enzyme site.

The p98/X2 clone represents a third polymorphic allele, having Thr at position 25 and Leu at position 58. The nucleotide sequence diverges from the other two clones at residue 1051, forming a complex pattern of inverted and direct repeats of upstream sequences (Fig. 3C). S1 nuclease protection analysis (*13*) showed the p90/135 transcript is the dominant, if not exclusive form expressed in IFN-γ–stimulated U937 cells (Fig. 3C). However, the existence of three polymorphisms among cDNAs obtained from one patient suggests there may be more than one gene encoding FcRI. The presence of a gene duplication is not excluded by the genomic blot hybridization data (*10*).

The predicted polypeptide sequences show the typical features of a type I integral membrane protein, and include a short hydrophobic signal sequence, a single 21-residue hydrophobic membrane–spanning domain, and a short, highly charged cytoplasmic domain (Fig. 4). The extracellular portion contains six potential N-linked glycosylation sites and six Cys residues distributed among three C2 set (*14*) Ig-related domains.

With the National Biomedical Research Foundation ALIGN program (*15*), quantitative sequence comparisons were made of the three immunoglobulin domains of FcRI and the two domains of the known low-affinity IgG receptors. High scores (expressed as standard deviations (SD) above the mean score for alignment of 50 random permutations of the two sequences) were calculated between the first domain of FcRI and the first domains of the human low-affinity FcRII (14.0 SD) and FcRIII (18.3 SD) receptors. Lower scores were obtained between the first domain of FcRI and the second domain of the low affinity receptors (FcRII, 7.2 SD and FcRIII, 6.4 SD). Similarly, high scores were observed between the second domain of FcRI and the second domains of low-affinity receptors (FcRII, 14.9 SD and FcRIII, 18.4 SD). The third FcRI domain showed little similarity to the other domains (comparison to the first domains: FcRII, 4.2 SD and FcRIII, 6.1 SD; and to the second domains: FcRII, 5.4 SD and FcRIII, 4.9 SD).

In summary, the extracellular region of FcRI consists of three Ig-like domains, two of which are highly related to the two Ig domains of FcRII and FcRIII. The third, less closely related domain may confer the high-affinity for IgG_1. In support of this, recent preliminary studies have shown that point mutations in the third domain of FcRI can result in decreased affinity for human IgG_1.

REFERENCES AND NOTES

1. C. L. Anderson and R. J. Looney, *Immunol. Today* **9**, 264 (1986); D. R. Burton, *Mol. Immunol.* **22**, 161 (1985); J. C. Unkeless, E. Scigliano, V. H. Freedman, *Annu. Rev. Immunol.* **6**, 251 (1988).
2. S. B. Halstead, *Science* **239**, 476 (1988); J. Homsy, M. Tateno, J. A. Levy, *Lancet* **i**, 1285 (1988).
3. V. A. Lewis, R. Koch, H. Plutner, I. Mellman, *Nature* **324**, 372 (1986); J. V. Ravetch *et al.*, *Science* **234**, 718 (1986); M. L. Hibbs *et al.*, *Proc. Natl. Acad. Sci. U.S.A.* **83**, 6980 (1986); S. G. Stuart *et al.*, *J. Exp. Med.* **166**, 1668 (1987); M. L. Hibbs, L. Bonadonna, B. M. Scott, I. F. C. McKenzie, P. M. Hogarth, *Proc. Natl. Acad. Sci. U.S.A.* **85**, 2240 (1988); D. Simmons and B. Seed, *Nature* **333**, 568 (1988).
4. S. Stengelin, I. Stamenkovic, B. Seed, *EMBO J.* **7**, 1053 (1988).
5. B. Seed and A. Aruffo, *Proc. Natl. Acad. Sci. U.S.A.* **84**, 3365 (1987); A. Aruffo and B. Seed, *EMBO J.* **6**, 3313 (1987); *Proc. Natl. Acad. Sci. U.S.A.* **84**, 8573 (1987).
6. B. Hirt, *J. Mol. Biol.* **26**, 365 (1967).
7. C. L. Anderson *et al.*, *J. Biol. Chem.* **261**, 12856 (1986).
8. P. Guyre and M. Fanger, personal communication.

9. R. J. Looney, G. N. Abraham, C. L. Anderson, *J. Immunol.* **136**, 1641 (1986).
10. J. M. Allen, unpublished data.
11. Forty-eight hours after transfection with the p135, p90, and p98/X2 cDNAs, COS cells were detached in phosphate-buffered saline (PBS), 1 m*M* EDTA, and incubated with ligand for 30 min at 4°C in PBS, 5% nonfat milk, and 0.2% sodium azide. Bound and free fractions were separated by centrifugation through a 3:2 mixture of dibutyl:dioctyl phthalates. Data were corrected for contribution of nonspecific binding by subtraction of counts per minute (cpm) bound in the presence of 2.5×10^{-4}*M* total IgG.
12. P. Guyre, P. M. Morganelli, R. Miller, *J. Clin. Invest.* **72**, 393 (1983); K. C. Petroni, L. Shen, P. Guyre, *J. Immunol.* **140**, 3467 (1988).
13. One microgram each of p90 and p98/X2 was ^{32}P-labeled at the Bst EII site between domains 2 and 3 and hybridized in 80% formamide, 0.4*M* NaCl and 10 m*M* 2-(*N*-morpholino)propanesulfonic acid (MOPS), *p*H 7.5, with 20 μg of total RNA at 50°C for 3 hours. After S1 nuclease digestion, samples were run on a 1.5% agarose gel and autoradiographed.
14. A. F. Williams and A. N. Barclay, *Annu. Rev. Immunol.* **6**, 381 (1988).
15. M. O. Dayhoff, W. C. Barker, L. T. Hunt, *Methods Enzymol.* **91**, 524 (1983).
16. Abbreviations for the amino acid residues are: A, Ala; C, Cys; D, Asp; E, Glu; F, Phe; G, Gly; H, His; I, Ile; K, Lys; L, Leu; M, Met; N, Asn; P, Pro; Q, Gln; R, Arg; S, Ser; T, Thr; V, Val; W, Trp; and Y, Tyr.
17. F. Sanger, S. Nicklen, A. Coulson, *Proc. Natl. Acad. Sci. U.S.A.* **74**, 5463 (1977).
18. We thank D. Simmons, M. Bevilacqua, A. Peterson, and N. Hogg for discussions and communication of unpublished information, C. Anderson for human IgG_3, and C. Anderson, P. Guyre and M. Fanger for MAbs 32.2, 22.2, and IV.3. J.M.A. is the recipient of a Wellcome Trust fellowship. Supported by a grant from Hoechst AG.

8 August 1988; accepted 1 November 1988

The Involvement of Platelet Activating Factor in Ovulation

AKINWUNMI O. ABISOGUN, PIERRE BRAQUET, ALEX TSAFRIRI*

Follicle rupture during ovulation is associated with inflammation-like changes. Because platelet activating factor (PAF) participates in the inflammatory process, the effect of a PAF-specific antagonist, BN52021, on the ovulatory response was tested in rats. BN52021, administered locally, inhibited follicle rupture in rats stimulated to ovulate with human chorionic gonadotropin (hCG). In addition to suppressing rupture of the follicles, this antagonist suppressed the hCG-stimulated increase in ovarian collagenolysis and vascular permeability. The inhibition of ovulation of BN52021 could be reversed by simultaneous administration of PAF. Furthermore, PAF partially reversed the blockage of ovulation by inhibitors of eicosanoid synthesis. Collectively, these results suggest the involvement of PAF in ovulation. Its role seems to be closely related to the metabolism of arachidonic acid. Thus, modulation of PAF action may serve as an additional target for regulation of reproduction via its action on ovulation.

THE RUPTURE OF MATURE OVARIAN follicles during ovulation involves changes that are also common to inflammation (*1*). Thus, induction of ovulation by gonadotropins, which stimulate increases in follicular tissue–type plasminogen activator (tPA) (*2*) and collagenase (*3, 4*) activities, can be blocked by inhibitors of the cyclooxygenase (*5*) and lipoxygenase (*6*) pathways or arachidonic acid (AA) metabolism. Recently, platelet aggregation and adherence to endothelial cells was observed in periovulatory ovine follicles (*7*). Likewise, margination of platelets in acutely inflamed tissues (*8*) and their high content of mediators, including vasoactive amines and peptides, proteases, chemotactic factors, and growth factors (*9*) were described. These findings prompted us to examine the possible involvement of the platelet activating factor [PAF; 1-*O*-octadecyl (or hexadecyl)-2-acetyl-glycero-3-phosphorylcholine] (*10*) in follicular rupture during ovulation.

Immature, 25- or 26-day-old female Wistar-derived rats were primed with 15 IU of pregnant mare's serum gonadotropin (PMSG) to produce multiple preovulatory follicles. Ovulation was induced with a subcutaneous injection of 4 IU of human chorionic gonadotropin (hCG) 48 to 54 hours after PMSG administration. Approximately 18 to 20 hours after administration of hCG, the rats were killed by cervical dislocation. The ampullae of the oviducts were excised, and the ovulated ova were released and counted under a dissecting microscope. When ovulation was inhibited, the presence of large Graafian follicles was confirmed by examination of the ovaries. The data of unilateral injections into the ovarian bursa were expressed as percent inhibition of the number of ovulated eggs in the oviduct of the treated versus the untreated side.

The involvement of PAF in ovulation was tested by injection of a specific PAF antagonist BN52021 (*11*) [median inhibitory concentration (IC_{50}), $10^{-7}M$], isolated from the Chinese tree *Ginkgo biloba L.* (*10, 12*). Unilateral injection of the antagonist into the ovarian bursa resulted in a dose-dependent inhibition of follicle rupture from the treated ovary (Table 1). The drug effectively blocked ovulation when administered concomitantly with hCG (0 time), or up to 9 hours after hCG treatment. The inhibition of follicle rupture was prevented when BN52021 (0.75 mg) and PAF (Sigma) were injected into the ovarian bursa simultaneously with hCG (Table 1). Administration of PAF (0.5 to 20 μg per bursa) to rats that were not stimulated by hCG and had their endogenous surge of luteinizing hormone (LH) blocked by Nembutal failed to induce ovulation.

In view of the action of inhibitors of eicosanoid synthesis on follicle rupture (*5,*

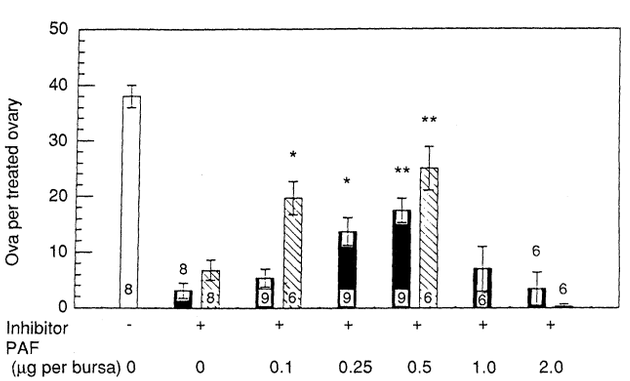

Fig. 1. Induction of ovulation by PAF in rats blocked by inhibitors of eicosanoid synthesis. Immature 25- or 26-day-old rats were injected with 15 IU of PMSG. After 48 to 50 hours, ovulation was stimulated by hCG (4 IU); 3 hours later indo (0.5 mg per bursa, solid bars) or NDGA (0.5 mg per bursa, hatched bars) and PAF were administered simultaneously in 50% dimethyl sulfoxide in saline (v/v) into one ovarian bursa. Ovulation was examined the next morning. Only the number of ova (mean ± SEM) released from the treated ovary are given; the untreated ovaries were not affected significantly by PAF. The number of rats is indicated on the bars. $*P < 0.01$; $**P < 0.001$ versus the rats treated with the same inhibitor only. Analysis of variance revealed a significant ($P < 0.001$) effect of PAF doses on inhibition of ovulation by indo or NDGA. Blank bar, control.

A. O. Abisogun and A. Tsafriri, Department of Hormone Research, Weizmann Institute of Science, Rehovot 76100, Israel.
P. Braquet, Institute Henri Beafour, 92350 Le Plessis Robinson, France.

*To whom correspondence should be addressed.